Molecular Dynamics Simulations of the Helical Antimicrobial Peptide Ovispirin-1 in a Zwitterionic Dodecylphosphocholine Micelle: Insights into Host-Cell Toxicity

Himanshu Khandelia[†] and Yiannis N. Kaznessis*[,†,‡]

Department of Chemical Engineering and Materials Science and The Digital Technology Center, University of Minnesota, 421 Washington Avenue Southeast, Minneapolis, Minnesota 55455

Received: January 10, 2005; In Final Form: March 18, 2005

We have carried out a 40-ns all-atom molecular dynamics simulation of the helical antimicrobial peptide ovispirin-1 (OVIS) in a zwitterionic diphosphocholine (DPC) micelle. The DPC micelle serves as an economical and effective model for a cellular membrane owing to the presence of a choline headgroup, which resembles those of membrane phospholipids. OVIS, which was initially placed along a micelle diameter, diffuses out to the water−DPC interface, and the simulation stabilizes to an interface-bound steady state in 40 ns. The helical content of the peptide marginally increases in the process. The final conformation, orientation, and the structure of OVIS are in excellent agreement with the experimentally observed properties of the peptide in the presence of lipid bilayers composed of 75% zwitterionic lipids. The amphipathic peptide binds to the micelle with its hydrophobic face buried in the micellar core and the polar side chains protruding into the aqueous phase. There is overwhelming evidence that points to the significant and indispensable participation of hydrophobic residues in binding to the zwitterionic interface. The simulation starts with a conformation that is unbiased toward the final experimentally known binding state of the peptide. The ability of the model to reproduce experimental binding states despite this starting conformation is encouraging.

Introduction

Less than two decades ago, Michael Zasloff fortuitously discovered the first helical antimicrobial peptide (AMP), magainin, in the skin of the frog *Xenopus laevis*. Since then, hundreds of other such peptides have been discovered from a plethora of living organisms, and many have been synthesized in laboratories with the aim of designing active molecules to combat antibiotic-resistant bacterial strains.[1,2] Indeed, our knowledge and comprehension of how helical AMPs function to kill microbial cells by nonspecific disruption of the plasma membrane lipid bilayer has improved drastically over this period. It is now understood that although helical AMPs are vastly different in sequence and functional activity, most peptides share characteristics such as cationic charge and amphipathic structure.[3] The role of arginine and lysine residues in binding to anionic bacterial cell envelopes has been proven, and the importance of hydrophobic residues in the interaction with the hydrophobic core has also been established.[4] The initial excitement about the use of AMPs in the clinic was tempered by cognizance of the toxicity of most native peptides toward host cells.[5] This drawback has led to numerous attempts to fine-tune many active peptides to reduce host-toxicity levels and improve specificity toward pathogenic cells. The effort has been largely guided by the general principle that within acceptable limits, increase of positive charge and lowering of hydrophobic content improves specificity of peptides. Magainin[6−8] is a typical example that has been subject to such studies.

However, the success of such point-mutation approaches has been largely limited, mainly because the underlying molecular mechanism of action of cell lysis is still not understood completely. Indeed, these mutations must induce many other significant global changes in the biophysical characteristics of the peptides, the molecular details of which are not well understood and are not accessible by experiments. The barrel-stave, carpet, and toroidal-pore models have been proposed to explain peptide-induced cell lysis macroscopically,[3] but a microscopic comprehension has been restricted because of the limitations of experimental methods to probe the fast dynamics of peptide−membrane interactions.

Many molecular dynamics (MD) simulations of peptides (not just AMPs) with model lipid assemblies have been carried out in the past few years to offer an answer to these problems. For reviews, please see refs 10, 11, and 12. Simulations do afford a vibrant molecular picture of peptide−membrane interaction that has consistently supplemented the limited experimental information. However, the constraints on current computational capabilities restrict large simulations to the order of tens of nanoseconds on the average. This time is palpably insufficient to sample the entire configurational phase space. The simulations are thus initialized based on a prior knowledge of the orientation and position of the peptide with respect to the interface, so that the starting assembly is as close to equilibrium configuration as possible. All-atom MD simulations where the starting conformation is far from the experimentally observed conformation may not converge to the correct equilibrium state in phase space. The restriction on the accessible time scales and the need for prior knowledge of binding conformations have hampered the predictive ability of these simulation efforts and this has attracted criticism that many such simulations are only of academic value. Simulations of absorption of helical peptides from the aqueous phase into the interface[9−11] have been partly successful in eliminating this shortcoming. Even in this simulation, the helical face on which the peptide binds depends on

* Author to whom correspondence should be addressed. E-mail: yiannis@cems.umn.edu.
[†] Department of Chemical Engineering and Materials Science.
[‡] The Digital Technology Center.

10.1021/jp050162n CCC: $30.25
Published on Web 06/10/2005

what part of the helix faces the interface in the starting simulation assembly. Most peptide−membrane simulations where the peptide is initially placed in the aqueous phase or at the interface suffer from these drawbacks. Additionally, the area per lipid in model phospholipid bilayers relaxes on the order of tens of nanoseconds, and the response of the bilayers to peptide insertion is relatively sluggish.[10] Single simulations of peptides in bilayers consume immense computational resources, and this is why there are only scattered efforts of simulations of AMPs with lipid bilayers. In the current study, we have carried out long-time-scale molecular dynamics simulations of a helical AMP ovispirin-1 in a dodecylphosphocholine (DPC) micelle in an attempt to understand the molecular mechanism of action of the peptide and to develop a model that can alleviate some of the above shortcomings. As explained in the Methodology section, our starting conformation has no obvious bias toward the final peptide conformation.

Ovispirin-1 (OVIS) is an 18-amino-acid helical derivative of the 29-residue helical cathelicidin bovine antimicrobial peptide, SMAP-29.[12] OVIS (KNLRR IIRKIIHIIKKYG) was found to have significant antimicrobial activity against both gram-positive and gram-negative bacteria over a wide range of salt concentrations.[12] The peptide is highly amphipathic and carries a charge of +7. However, ovispirin-1, like SMAP-29, is unsuitable for therapeutic use owing to its hemolytic properties, which cause large-scale damage to human erythrocytes and epithelial cells.[12] Although nontoxic single-residue mutants (novispirin-G10 and novispirin-T7) of OVIS have been designed,[13] the biophysical properties of the peptide that result in toxicity have not been rationalized.

The DPC[14] micelle has been successfully modeled for MD simulations in CHARMM (Chemistry at Harvard Macromolecular Mechanics).[15] Simulations of micelles of various anionic and zwitterionic lipid micellar systems[14,16−26] have been successfully used to interpret and supplement the information obtained from experimental methods. In the past few years, simulation force fields such as CHARMM,[15] AMBER,[27] and GROMACS[28] have been fairly well parametrized to accurately simulate hydrated lipid assemblies. The current study focuses on the initial events involved in peptide binding on the micellar surface, the state of the peptide secondary structure, and the role that specific amino acids play in bringing about the final binding states.

The primary advantage of using micelles as opposed to lipid bilayers is the faster time scales of motion of DPC lipids. It has been shown both by experiment[29] and by molecular dynamics simulations[14,21−23] that the slowest relaxation times of lipids in micellar solutions are of the order of 500−2000 ps. The only exception to these are the slower relaxation times of counterions.[18] The interaction of the peptide with the lipid macromolecular assembly induces a much faster response in micelles as opposed to bilayers. The micelle contains about half the number of atoms of a typical 128-lipid peptide−water-bilayer simulation cell. This allows much longer simulations and permits monitoring of biological phenomena of longer time scales. The geometry of the micelle permits setting up of a relatively less biased simulation (Methodology section). Additionally, sometimes the simulation results can be directly compared to the experimental structures of the peptide, which are often determined in the presence of SDS and DPC detergent micelles. The disadvantages of having a spherical (instead of a planar) interfacial geometry are more than offset by the expediencies offered by micellar models for the sake of the current study, which mainly addresses the details of peptide−membrane binding states.

The helical structure of most AMPs is membrane-induced, and the peptides themselves are known to be unstructured in solution. In principle, the starting structure of the peptide should not be helical in a membrane-binding simulation with the peptide starting in the aqueous phase. However, the time scales of folding of peptides on interfaces are too long to be accessed by large all-atom simulations. Thus, as noted by Kandaswamy and Larson,[11] such simulations are compelled to begin with the peptide being in the unnatural helical form in the aqueous phase. This enables the convergence of the simulation to a stable membrane-bound helical peptide conformation that can be compared to experimental results. In contrast, we begin our simulations with the peptide placed inside the membrane core. Our simulation thus suffers less from these shortcomings.

Methodology

The starting coordinates of the DPC micelle−water complex were obtained from simulations carried out by Wymore et al.[14] This structure was obtained after extensive minimization and dynamics of about 1 ns in a cubic simulation cell. We placed the micelle consisting of 60 DPC molecules and 4377 water molecules in a cubic simulation box of cell size 56.15 Å. The cell dimensions were set up to obtain the equilibrium bulk water density (0.033 $Å^{-3}$) far away from the interface.

Water was modeled using the TIP3P potential.[30] Seven chloride counterions and five Na^+ and Cl^- ions as 0.15 mM electrolyte were randomly distributed in the aqueous phase. The initial structure of OVIS was obtained from the PDB databank (PDB code 1HU5). Solid-state NMR experiments of OVIS[31] in lipid bilayers suggest that the majority of the OVIS helix is oriented parallel to the interface. However, we did not place the peptide initially at the DPC−water interface to avoid biasing the simulation toward the correct final conformation. Instead, the peptide was placed in the simulation box with its center of mass coinciding with that of the micelle. In this conformation, the peptide helical axis lay along one of the diameters of the micelle, with only its termini exposed to the solvent interface (Figures 2a and 2c). Owing to spherical symmetry of the micelle, the orientation of the peptide is unimportant, and there is no preferential bias as to which face of the peptide will (eventually) bind the interface. The fast dynamic time scales of DPC molecules ensured that the repositioning of the peptide to its final conformation would be computationally tractable.

To remove initial bad contacts between the peptide and the DPC core and prevent penetration of water, the peptide and bulk water were kept under weak harmonic constraints with spring constants of 10 and 5 kcal mol^{-1} $Å^{-1}$, respectively, during equilibration. The constraints were gradually removed in 20 000 steps of minimization (steepest descent method). The entire system was then minimized for 20 000 more steps without any constraints. Thereafter, the system consisting of ∼16 000 atoms was gradually heated to 303 K. The entire assembly was subjected to *NPT* dynamics at pressure $P = 1$ atm and temperature $T = 303.15$ K for 39 ns. The constant pressure/temperature module of CHARMM was used for the simulation with a leapfrog integrator. A time step of 2 fs was used. The temperature was set at 303.15 K using Hoover temperature control.[32] For the extended system pressure algorithm employed, all of the components of the piston mass array were set to 500 amu.[33] The electrostatic interactions were simulated using the particle mesh Ewald (PME) summation[34,35] without truncation and a real space Gaussian width of 0.25 $Å^{-1}$, a β-spline order

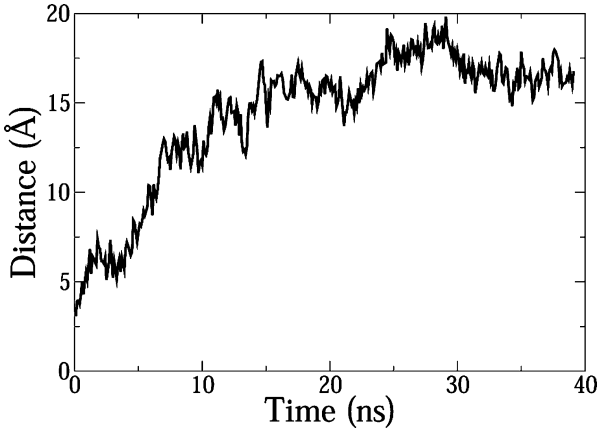

Figure 1. Distance between the center of mass of the peptide and the DPC micelle. Data collected every 4 ps.

of 4, and a fast Fourier transform grid of about 1 point per Å. SHAKE was used to eliminate the fastest degrees of freedom involving bonds with hydrogen atoms. The simulation was carried out using CHARMM, version c30b2, with the all-atom param22 parameter set. The simulation was run on parallel processors on the Marvel Tru64 Unix clusters at the Pittsburgh Supercomputing Institute and on the SGI Altix linux-based platforms at the Minnesota Supercomputing Institute. Because the equilibrium steady state was reached after 30 ns (see below), ensemble average properties were calculated for the last 9 ns of the simulation. For calculation of most dynamic properties, trajectories were sampled every 4 ps.

Results and Discussion

Peptide Position and Orientation. During the first 30 ns of simulation, OVIS diffuses from the micellar core to the interfacial region of the micelle and remains bound to the interface for the rest of the simulation.

Figure 1 shows how the peptide moves away from the center of mass of the micelle. Within the first 20 ns of simulation, there are several short simulation periods of 3−4 ns when the peptide does not translate. However, once the peptide reaches the interface, there is no indication of a new conformation, position, or orientation for a further ∼9 ns of simulation. We can safely conclude that the interface-bound conformation of the peptide corresponds to its equilibrium state in the presence of the DPC membrane mimetic. As described in the Methodology section, we took care to start the simulation with a peptide conformation that was far from the experimentally predicted configuration to avoid methodological bias.

Solid-state NMR[31] and the proton inverse detected deuteron (PRIDE) NMR technique[36] indicate that ovispirin prefers to bind nearly parallel to the membrane−water interface (this corresponds to the final simulation conformation) and is not positioned across the bilayer (this corresponds to the starting simulation configuration). In both experiments, the peptide was reconstituted in lipid vesicles composed of (POPC: palmitoyl-oleoyl-phosphatidylcholine, POPG: palmitoyl-oleoyl-phosphatidylglycerol) lipids in a 3:1 ratio. Thus, the final peptide position (Figure 2) from the simulation agrees very well with the experimentally predicted binding.

The driving force behind the diffusion is the amphipathic structure of OVIS. Figure 3d is a helical wheel diagram of the peptide. In helical form, OVIS has a conspicuous segregation of polar and nonpolar residues into two topological halves. In isolation from other peptides, a strongly amphipathic helix like OVIS is more prone to bind to the interfacial region, with its

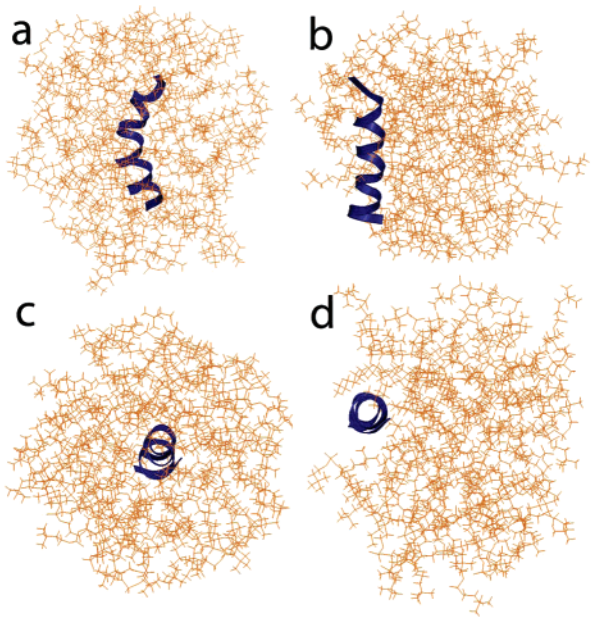

Figure 2. Initial (left) and the final (right) conformations of the simulation. Parts a and b are side views, while parts c and d are top views. Snapshots were taken at the $t = 0$ and $t = 39$ ns.

hydrophobic face embedded in the membrane core, and the polar helical region exposed to the solvent and/or interacting with the lipid headgroups. Yamaguchi et al.[31] proposed a similar model from NMR experiments. The equilibrium average binding conformation of OVIS is in agreement with the experimentally predicted orientation of the peptide (Figure 3). The hydrophobic face is immersed in the lipid core in the equilibrium-averaged conformations, while the polar face is exposed to the interfacial headgroups and solvent. Thus, with respect to the peptide's equilibrium position and its orientation relative to the membrane interface, the simulation results agree with experimental observation.

Peptide Structure. In the presence of trifluoroethanol (TFE), OVIS is a uniform helix from residues 4 to 16.[13] This peptide structure was used to start the simulation. The core of the peptide is in a completely hydrophobic environment. With only the termini of the peptide exposed to the interface, the backbone C═O and N−H atoms at positions i and $i + 4$ form stronger intramolecular hydrogen bonds to offset the entropic costs associated with exposed hydrophilic groups in the micellar core. This results in a marginal increase in the helical content of the peptide as the simulation progresses. Figure 4 shows the ensemble-averaged dihedral angle (φ,ψ) values.

Relative to the PDB structure in TFE, the average dihedral angles in the simulation confirm more strictly to the Ramachandran plot values of (−60,−50). The formation of a tighter helix goes hand in hand with the increased amphipathicity of the peptide. This favors the interface-bound state where the hydrophobic helical face remains deeply inserted in the micellar core. Other than the unconstrained terminal positions, the dihedral angle at position 13 deviates most from the (−60,−50) values. NMR experiments do suggest the possibility of formation of a C-terminal bend in OVIS when bound to bilayers.[31] This might be manifest in the slight deviation at position 13. However, this deviation is only on the order of ∼10° and is comparable to the magnitude of the fluctuations (error bars in Figure 4). Thus, it is not possible to interpret it as a bend in the helix. It is of note that the zwitterionic interface prevents deformations in structure that are rendered possible near an anionic interface due to strong electrostatic peptide−

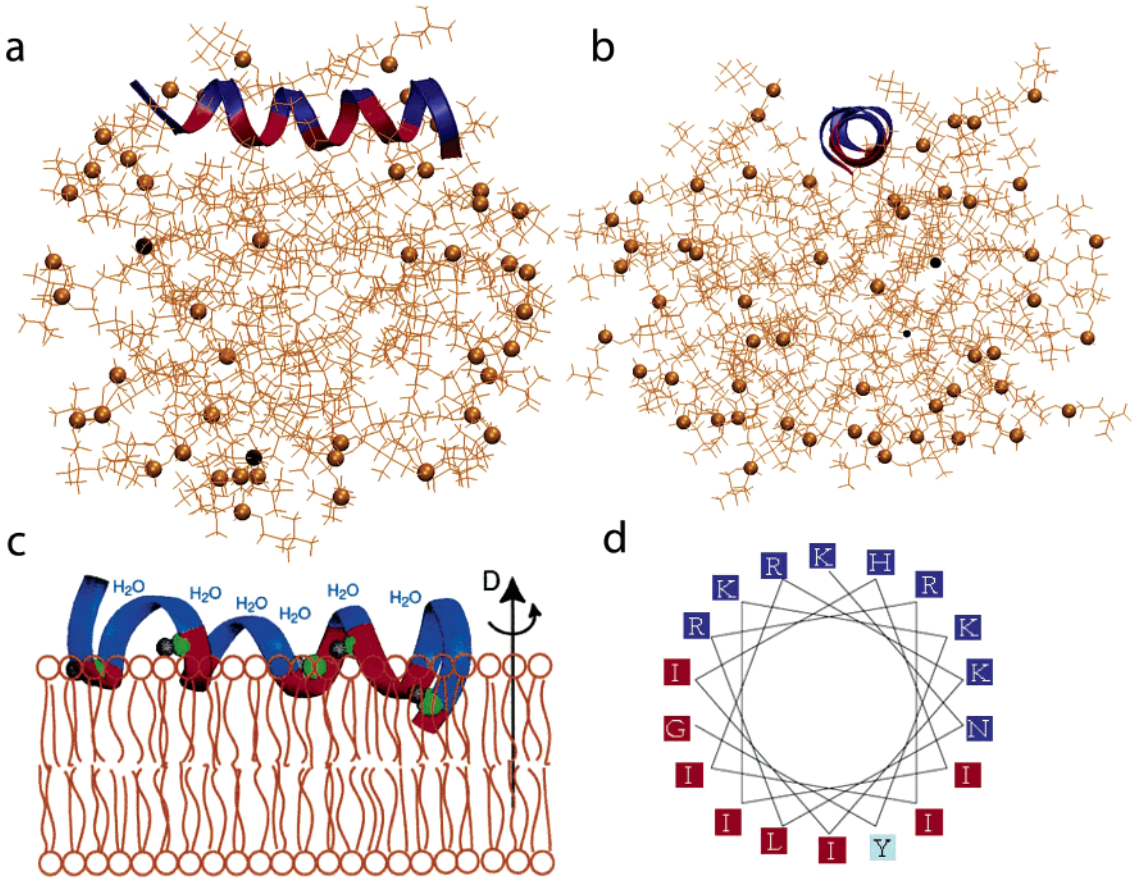

Figure 3. (a and b) Final conformation of the peptide relative to the micelle. (c) Binding of OVIS as predicted by NMR. (Reprinted with permission from ref 31. Copyright 2001 the Biophysical Society.) (d) Helical wheel diagram of OVIS. In all four panels, hydrophobic residues are shown in red, polar residues in blue.

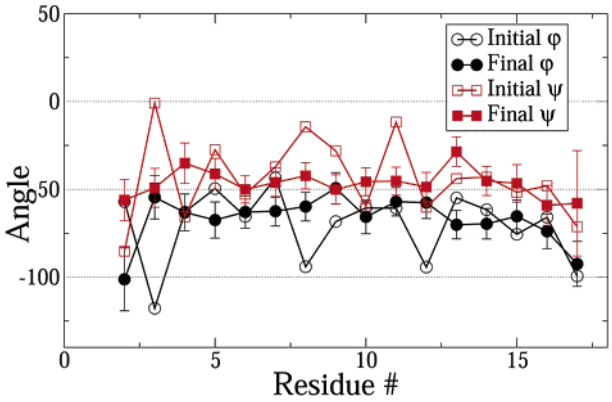

Figure 4. Dihedral angles of the peptide. The open boxes and circles are angles calculated from the PDB structure. The closed boxes and circles are ensemble averages.

micelle forces. The NMR experiments were carried out in the presence of 25% anionic lipid. Additionally, any significant perturbation of the helix is prevented by the rigidity induced in the peptide by the strong affinity of the hydrophobic helical region to the DPC micellar core.

Given that PME has been used for electrostatic calculations, there is the possibility of periodicity-induced artifacts in helix stability. Weber et al.[37] observed the retention of artificial helicity of an eight-amino-acid peptide in 2-ns simulations in explicit solvent using a lattice-sum method to calculate long-range electrostatics. However, the structure and dynamics of a DNA dodecamer in explicit solvent in a 1.5-ns simulation were unaffected by the size of the unit cell.[38] Although the relevance of lattice-sum artifacts in simulations of large biomolecular complexes in explicit solvent is still a moot question,[39] the possibility of the helix stability being a periodicity-induced artifact cannot be completely ruled out. This is mainly because the extent of solvent screening on direct Coulombic interactions is limited in the current simulation owing to the low dielectric constant of the micelle. The minimal distance between the peptide and the periodic box boundaries is about 8 Å in the final peptide conformation. We ensure that the bulk water density of 1 g cm^{-3} is achieved at the unit cell boundaries.

Backbone Hydrogen-Bonding Patterns. Often, a disruption of the helical peptide structure in the presence of an interface might be accompanied by the concurrent formation of hydrogen bonds between the peptide backbone and the interfacial hydrogen bond donors and acceptors.[19] We counted the number of hydrogen bonds formed by the backbone carbonyl oxygen and the backbone amide hydrogen atoms with the DPC headgroups. In accordance with the stability of the helix in the simulation, none of the peptide backbone atoms (except the first three residues at N-terminus) forms hydrogen bonds with the DPC molecules. The termini backbone atoms do form hydrogen bonds with water, but these bonds are transient and result from the temporary proximity of a water molecule near the peptide donor/acceptor atom.

A concern with the use of the param22 (and the param27) parameter set of CHARMM is the tendency of the force field to favor the formation of unnatural π-helices in the solvated state.[40−42] We have used the param22 parameter set and have confirmed that the π-helix does not form in our simulations. Please see the Appendix for a detailed analysis and discussion.

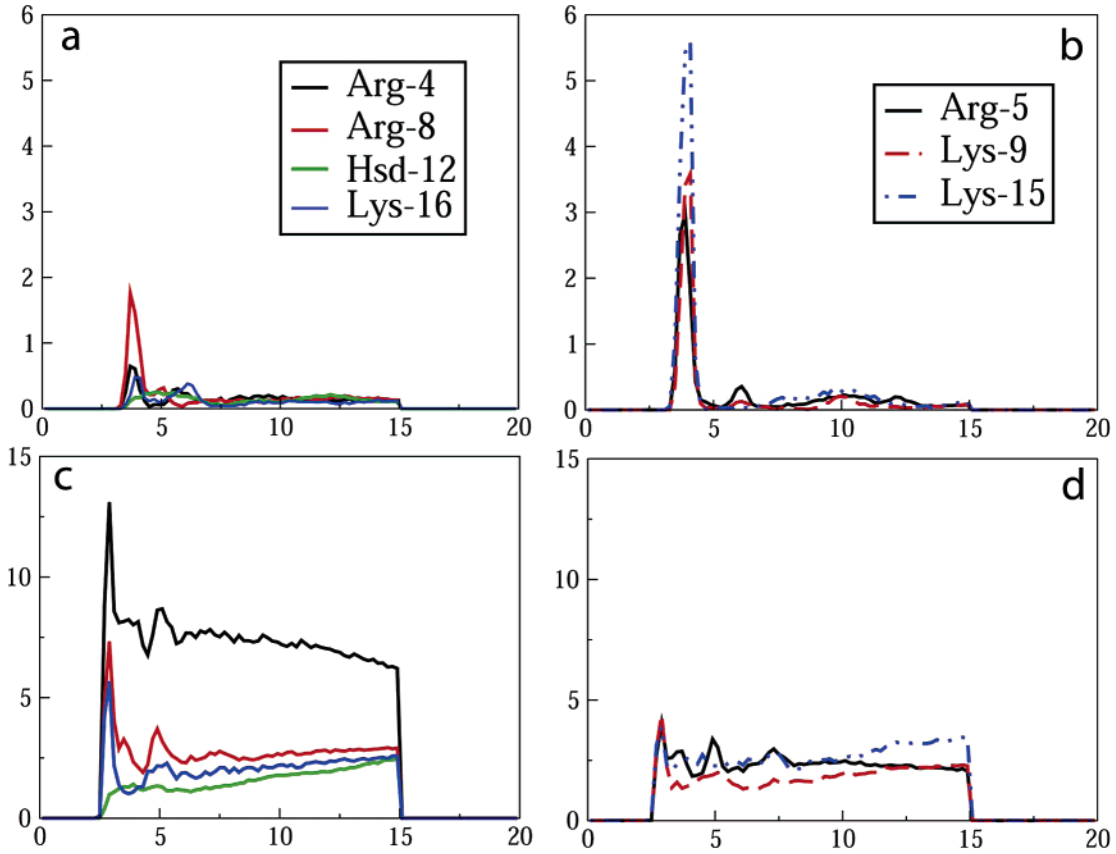

Figure 5. Radial distribution functions of the side chain heavy atoms of polar amino acids the peptide: (a and b) with respect to phosphorus atoms of the DPC lipids; (c and d) with respect to water. Trajectories were sampled every 12 ps.

Peptide−Micelle and Peptide−Water Interactions. To analyze the molecular structural details of peptide−micelle binding, we have calculated radial distribution functions between specific chemical moieties on the peptide and the micelle. These calculations inform us of the detailed location and orientation of the peptide with respect to the micelle as well as provide knowledge about hydrogen-bond-formation patterns and hydrophobic interactions.

The polar half of the OVIS helix has three arginine and four lysine residues. Each of these is capable of forming hydrogen bonds. Additionally, asparagine at position 2, histidine at position 12, and the tyrosine residue at position 17 can afford donor and acceptor atoms for (relatively weaker) hydrogen-bond formation. The DPC headgroup carries a highly electronegative phosphate center comprised of four strong hydrogen-bond acceptor oxygen atoms. Although the DPC micelle is zwitterionic, the phosphates do bind the positively charged peptide side chains. This binding is driven by both hydrogen-bond-formation disposition and plain electrostatic attraction. We calculated radial distribution functions (RDFs) between the polar side chains of the peptide and the phosphate atom of the DPC lipids. The guanidium ions on the side chains were used to construct the RDFs in case of arginine and lysine.

All lysines and arginines form well-defined peaks at $r = 4$ Å, indicating the formation of stable hydrogen bonds. Note that the RDFs were not drawn with the donor and acceptor atoms themselves; hence the peak is at ∼4 Å instead of the hydrogen-bonding distance of 3 Å.

Residues Arg4, Arg8, His12, and Lys16 (set 1) all have smaller peaks compared to those of the other positively charged residues Arg5, Lys9, and Lys15 (set 2). The lower values of $g(r)$ signify that residues 4, 8, 12, and 16 form weaker hydrogen bonds with DPC. Interestingly, these residues form intramolecular i and $i + 4$ backbone hydrogen bonds with each other and are thus spatially segregated to the same region in space. The weaker interaction of these residues with DPC lipids indicates that more often than not their side chains point into the aqueous phase and will be more hydrated compared to residues of set 2. (RDFs drawn against the DPC lipid aliphatic chain atoms indicate that they do not point into the micellar core.) To quantify the extent of hydration of the side chains, RDFs were drawn with the water molecules. Indeed, the side chains of the set 2 residues are less hydrated than those of set 1, as is shown in Figures 5c and 5d. However, all polar residues, except histidine, have well-hydrated side chains.

Although the peptide is localized on the interface, the backbone and side chains of the peptide are hydrated to different extents. The peptide-induced micellar shape as shown in Figure 2 is ellipsoidal. The cylindrical peptide body resides at the bottom of a gently sloping cavity formed by the DPC lipids around the peptide. This leads to a highly eccentric micelle, unlike those seen in previous simulations of peptides in micelles. The side chains of nonpolar lipids protrude into the micellar core while the side chains of polar lipids protrude into the aqueous phase and are well-hydrated (Figures 5c and 5d). However, the peptide backbone is rigidly bound to the DPC lipids near the bottom of the trough, and not the entire backbone is hydrated. Calculations of hydration numbers at a radius of 3.8 Å about the Cα atoms revealed that only the N-terminal and C-terminal residues are well-hydrated on their backbones. The central region of the peptide (residues 6−14) has low backbone hydration. Interestingly, all of the Ile residues (7, 10, 11, 13, and 14) are clustered in this part of the helix. The

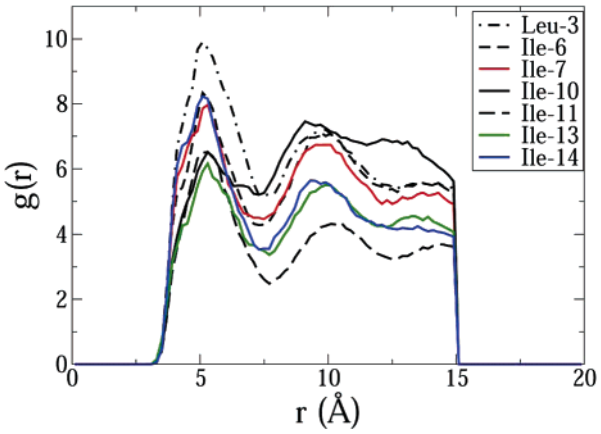

Figure 6. Radial distribution functions of side chain heavy atoms of hydrophobic residues and the aliphatic DPC carbon atoms.

evidence here points to strong hydrophobic binding between these isoleucine residues and the micellar core.

RDFs constructed between the side chains of hydrophobic residues with the lipid aliphatic carbons further confirm this binding (Figure 6). This force keeps the peptide tightly bound to the micelle in the trough. As is evident from Figure 6, most of the hydrophobic residues show a strong affinity to the aliphatic phase.

The observations made here directly testify to the hypothesis that the hydrophobic forces of entropic nature make a large contribution to the overall binding free energy of the peptide. This binding becomes significant in the current simulation because the electrostatic peptide−micelle binding enthalpy is lower in zwitterionic lipids as compared to anionic lipids. The mutations in both T7 and G10 involve the replacement of an isoleucine by a less hydrophobic reside (threonine in T7 and glycine in G10). The mutant peptides will thus have a reduced hydrophobic contribution to the binding free energy. This leads to these peptides having lesser affinity toward zwitterionic interfaces, which in turn implies reduced toxicity. As discussed before, substituting hydrophobic residues with polar ones has been one of the central guiding principles for AMP mutations.

Conclusions

We have carried out long-time simulations of a helical antimicrobial peptide in a zwitterionic lipid micelle. Despite starting from a configuration far from the expected final state, the simulation converges to the correct experimentally observed binding conformation of the peptide.

We have quantified the different types of interactions of the OVIS peptide with the DPC micelle and water that lead to peptide toxicity against host cells. The simulation suggests that the association of hydrophobic peptide residues with the micellar core plays a pivotal role in hinging the peptide to the zwitterionic membrane. The central two coils of the peptide (residues 6−14) are rich in nonpolar residues. This region of the peptide remains less hydrated along its backbone owing to the preference of the amino acids to associate with the micellar core. This also results in the retention of a large percentage of peptide helical content. The side chains of polar residues are either involved in the formation of hydrogen bonds with the oxygen atoms on the phosphate groups or in the formation of hydrogen bonds with water. Interestingly, these two interactions are mutually exclusive. The polar side chains that bind phosphate ions are relatively less hydrated and vice versa.

The spherical geometry of the micelle prevents comparison to experimental order parameter data and also precludes the molecular-scale observation of the phenomena of positive or negative hydrophobic mismatch that might have a role in determining whether a peptide causes cell lysis in accordance with the barrel-stave, toroidal-pore, or carpet model.[3] Although not as appropriate a model for a real membrane as a lipid bilayer, the DPC micelle captures the essential features that modulate peptide−membrane interaction. These are the presence of a strongly hydrophobic core and a flexible polar interface capable of forming hydrogen bonds and salt bridges with the solvent and the peptide and also capable of responding dynamically to peptide−membrane interactions.

There are other advantages to using micelles. The simulations run more than 3 times as fast as a hydrated lipid bilayer peptide assembly, and the time scale of motions of DPC lipids are faster than those of zwitterionic membrane phospholipids (DOPC, DMPC, or DPPC). This enables the peptide to diffuse to the final binding conformation fast enough and the lipids to equilibrate about the peptide quickly. Additionally, the symmetry of the spherical micelle diminishes the extent of orientational bias that plagues simulations that are carried out in bilayers with the peptide placed in the aqueous phase. This also avoids the need to start the simulation from different initial configurations. Given its ability to correctly reproduce experimental binding states, we anticipate that this simulation setup can become useful when comparing dynamic binding properties of different helical peptides. Similar multiple simulations will be computationally too expensive to carry out in bilayers. The micelle simulations can set up a basis for generating comparative molecular-scale information that can be of help in interpreting experimental data and understanding atomic-scale physical interactions that result in slightly different peptides having different cytotoxic and antibacterial activities.

Acknowledgment. This work was supported by grants from IBM (Faculty award to Y.N.K) and 3M (Young Faculty award to Y.N.K). H.K. has an Amundson Fellowship at the department of Chemical Engineering and Materials Science, University of Minnesota. Computational support from the Minnesota Supercomputing Institute is gratefully acknowledged. This work was also partially supported by National Computational Science Alliance under MCB030027P and utilized the marvel cluster at the Pittsburgh Supercomputing Center.

Appendix

A concern with the use of the param22 (and the param27) parameter set of CHARMM is the tendency of the force field to favor the formation of unnatural π-helices in the solvated state.[40−42] In a π-helix, hydrogen bonds are formed between the C═O oxygen atom of the ith amino acid with the N−H hydrogen atom of the $(i + 5)$th amino acid, instead of an $i, i + 4$ motif as in the classical α-helix. This results in the formation of a more open helix with a higher entropic cost leading to an unfavorable free energy.[42] Normally, π-helices have been known to occur only in exceptional circumstances, but both atomistic and implicit simulations of helical peptides have been known to favor their formation in aqueous solution.[42] The CMAP: grid-based energy correction maps corrected param22 parameter set has been found to rectify this problem.[40−42] To our knowledge, the problem has not been detected in all-atom simulations of lipid−water biphasic systems yet. We used the classical param22 set for our work. To make sure that our simulation did not carry the π-helix artifact, we counted the fraction of backbone $i, i + 4$ and $i, i + 5$ hydrogen bonds. A hydrogen bond was considered to formed if the C═O···N−H distance was less than 3 Å and

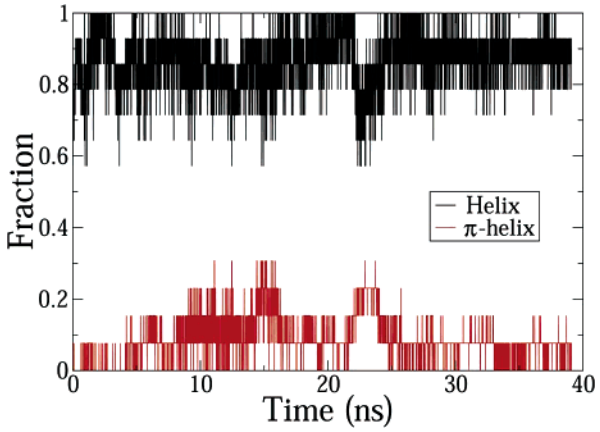

Figure 7. Fraction of backbone helical i, $i + 4$ (black) and π-helical i, $i + 5$ (red) hydrogen bonds. Data were collected every 4 ps.

the N−H−O angle was less than 120°. The results have been shown in Figure 7. Although there is a small fraction of hydrogen bonds that confirm to the π-helical state, the majority of the hydrogen bonds are consistent with the formation of a classical α-helix. In fact, there are extended periods of time when all of the i, $i + 4$ hydrogen bonds were satisfied, indicating the formation of a stable Ramachandran helix.

References and Notes

(1) Zasloff, M. *Nature* **2002**, *415*, 389.
(2) Brahmachary, M.; Krishnan, S. P.; Koh, J. L.; Khan, A. M.; Seah, S. H.; Tan, T. W.; Brusic, V.; Bajic, V. B. *Nucleic Acids Res.* **2004**, *32*, D586.
(3) Shai, Y.; Oren, Z. *Peptides* **2001**, *22*, 1629.
(4) Epand, R. M.; Vogel, H. J. *Biochim. Biophys. Acta* **1999**, *1462*, 11.
(5) Reddy, K. V.; Yedery, R. D.; Aranha, C. *Int. J. Antimicrob. Agents* **2004**, *24*, 536.
(6) Dathe, M.; Nikolenko, H.; Beyermann, M.; Bienert, M. *FEBS Lett.* **2001**, *501*, 146.
(7) Hallock, K. J.; Lee, D. K.; Ramamoorthy, A. *Biophys. J.* **2003**, *84*, 3052.
(8) Tachi, T.; Epand, R. F.; Epand, R. M.; Matsuzaki, K. *Biochemistry* **2002**, *41*, 10723.
(9) Shepherd, C. M.; Schaus, K. A.; Vogel, H. J. *Biophys J.* **2001**, *80*, 579.
(10) Shepherd, C. M.; Vogel, H. J.; Tieleman, D. P. *Biochem. J.* **2003**, *370*, 233.
(11) Kandasamy, S. K.; Larson, R. G. *Chem. Phys. Lipids* **2004**, *132*, 113.
(12) Kalfa, V. C.; Jia, H. V. P.; Kunkle, R. A.; McCray, P. B.; Tack, B. F.; Brogden, K. A. *Antimicrob. Agents Chemother.* **2001**, *45*, 3256.
(13) Sawai, M. V.; Waring, A. J.; Kearney, W. R.; McCray, P. B., Jr.; Forsyth, W. R.; Lehrer, R. I.; Tack, B. F. *Protein Eng.* **2002**, *15*, 225.
(14) Wymore, T.; Gao, X. F.; Wong, T. C. *J. Mol. Struct.* **1999**, *485*−*486*, 195.
(15) Brooks, B. R.; Bruccoleri, R. E.; Olfson, B. D.; States, D. J.; Swaminathan, S.; Karplus, K. *J. Comput. Chem.* **1983**, *4*, 187.
(16) Bruce, C. D.; Berkowitz, M. L.; Perera, L.; Forbes, M. D. E. *J. Phys. Chem. B* **2002**, *106*, 3788.
(17) Bruce, C. D.; Senapati, S.; Berkowitz, M. L.; Perera, L.; Forbes, M. D. E. *J. Phys. Chem. B* **2002**, *106*, 10902.
(18) MacKerell, A. D., Jr. *J. Phys. Chem.* **1995**, *99*, 1846.
(19) Wymore, T.; Wong, T. C. *Biophys. J.* **1999**, *76*, 1213.
(20) Wymore, T.; Wong, T. C. *J. Biomol. Struct. Dyn.* **2000**, *18*, 461.
(21) Wong, T. C.; Kamath, S. *J. Biomol. Struct. Dyn.* **2002**, *20*, 39.
(22) Tieleman, D. P.; van der Spoel, D.; Berendsen, H. J. C. *J. Phys. Chem. B* **2000**, *104*, 6380.
(23) Rakitin, A. R.; Pack, G. R. **2004**, *J. Phys. Chem. B* **2004**, *108*, 2712.
(24) Marrink, S. J.; Mark, A. E. *Biochemistry* **2002**, *41*, 5375.
(25) Gao, X.; Wong, T. C. *Biopolymers* **2001**, *58*, 643.
(26) Langham, A.; Kaznessis, Y. *J. Pept. Sci.* **2005**, *11*, 215.
(27) Pearlman, D. A.; Case, D. A.; Caldwell, J. W.; Ross, W. S.; Cheatham, T. E., III; DeBolt, S.; Ferguson, D.; Seibel, G.; Kollman, P. *Comput. Phys. Commun.* **1995**, *91*, 1.
(28) Berendsen, H. J. C.; van der Spoel, D.; van Drunen, R. *Comput. Phys. Commun.* **1995**, *91*, 43.
(29) Fernandez, P.; Schroedle, S.; Buchner, R.; Kunz, W. *ChemPhysChem* **2003**, *4*, 1065.
(30) Jorgensen, W. L.; Chandrasekhar, J.; Medura, J. D.; Impey, R. W.; Klein, M. L. *J. Chem. Phys.* **1983**, *79*, 926.
(31) Yamaguchi, S.; Huster, D.; Waring, A.; Lehrer, R. I.; Kearney, W.; Tack, B. F.; Hong, M. *Biophys. J.* **2001**, *81*, 2203.
(32) Hoover, W. G. *Phys. Rev. A* **1985**, *31*, 1695.
(33) Ryckaert, J.-P.; Ciccotti, G.; Berendsen, H. J. C. *J. Comput. Phys.* **1977**, *23*, 327.
(34) Darden, T.; York, D.; Pedersen, L. *J. Chem. Phys.* **1993**, *98*, 10089.
(35) Essmann, U.; Perera, L.; Berkowitz, M. L.; Darden, T.; Lee, H.; Pedersen, L. G. *J. Chem. Phys.* **1995**, *103*, 8577.
(36) Yamaguchi, S.; Hong, M. *J. Magn. Reson.* **1997**, *155*, 244.
(37) Weber, W.; Huenenberger, P. H.; McCammon, J. A. *J. Phys. Chem. B* **2000**, *104*, 3668.
(38) de Souza, O. N.; Ornstein, R. L. *Biophys. J.* **1997**, *72*, 2395.
(39) Kastenholz, M. A.; Huenenberger, P. H. *J. Phys. Chem. B* **2004**, *108*, 774.
(40) Freedberg, D. I.; Venable, R. M.; Rossi, A.; Bull, T. E.; Pastor, R. W. *J. Am. Chem. Soc.* **2004**, *126*, 10478.
(41) Mackerell, A. D., Jr.; Feig, M.; Brooks, C. L., III *J. Comput. Chem.* **2004**, *25*, 1400.
(42) Feig, M.; MacKerell, A. D., Jr.; Brooks, C. L., III *J. Phys. Chem. B* **2003**, *107*, 2831.